Regional cerebral blood flow decline can predict atrophy in Alzheimer's disease spectrum

Fardin Nabizadeh
Neuroscience Research Group (NRG), Universal Scientific Education and Research Network (USERN), Tehran, Iran

Mohammad Reza Rostami
Neuroscience Research Group (NRG), Universal Scientific Education and Research Network (USERN), Tehran, Iran

Mohammad Balabandian (balabandianm@gmail.com)
Neuroscience Research Group (NRG), Universal Scientific Education and Research Network (USERN), Tehran, Iran

Research Article

Keywords: Alzheimer's Disease, cerebral blood flow, atrophy, mild cognitive impairment

Posted Date: February 10th, 2021

DOI: https://doi.org/10.21203/rs.3.rs-151934/v2

Abstract

According to MRI findings, brain atrophy and structural changes play important roles as valid biomarkers for Alzheimer's Disease (AD) and can support the clinical diagnosis of AD. A decline in the regional cerebral blood flow (rCBF) is believed to be one of the initial changes in the AD continuum. Some studies revealed an association between the amyloid beta (Aβ) and rCBF pattern and suggested that reduced rCBF is an early consequence of neural death prior to considerable grey matter loss. Therefore, in the present study, we investigated the association between rCBF and brain structural changes in three groups of individuals, that is, control (CN), MCI, and AD groups. Our findings revealed a wide spread significant correlation between the rCBF and structural changes, including cortical volume, subcortical volume, surface area, and thickness in all groups after adjusting for age, sex, and APOE genotyping status. According to the present results, CBF might predict future structural changes and cause neurodegeneration associated with AD development, regardless of Aβ or tau accumulation.

Introduction

Alzheimer's disease (AD) is a neurodegenerative disease with symptoms, such as dementia, personality changes, and executive dysfunction (1). Physicians may use mental status examination and neuropsychological tests to assess the symptoms of these patients. Imaging methods, such as computed tomography (CT) and magnetic resonance imaging (MRI), are used to rule out other probable causes of dementia (2). However, these modalities are not adequate to diagnose AD because of the overlaps with normal aging changes in the brain.

According to MRI findings, brain atrophy and structural changes play important roles as valid biomarkers for AD (3, 4) and can support the clinical diagnosis of AD (5). Based on previous studies, it can be concluded that the rate of whole-brain atrophy is an excellent biomarker to predict the progression of AD in patients with mild cognitive impairment (MCI) (6). AD patients typically show atrophy in the medial temporal lobe (7), entorhinal cortex (8), and posterior cingulate cortex (9). According to the findings of a study by Benjanin et al., structural changes are associated with hypometabolism in the large posterior neocortical regions of the brain in AD patients (10).

Generally, atrophy in the brain has been reported in a vast majority of neurological diseases. According to previous studies, there is a significant correlation between the pattern of atrophy and Parkinson's disease (11, 12) and amyotrophic lateral sclerosis (ALS) (17). Therefore, the atrophy in MRI, could be a reliable biomarker to discriminate AD from other neurodegenerative diseases in the early onset of the disease. Evidence shows that amyloid-beta (Aβ) and tau protein, as the principal molecular changes in the AD pathology, are responsible for changes in the brain structure (13).

A decline in the regional cerebral blood flow (rCBF) is believed to be one of the initial changes in the AD continuum (14). However, the cause of this reduction is not fully understood yet. In this regard, N. Mattsson et al. revealed an association between the amyloid beta (Aβ) and rCBF pattern and suggested

that reduced rCBF is an early consequence of neural death prior to considerable grey matter loss (15). Therefore, in the present study, we investigated the association between rCBF and brain structural changes in three groups of individuals, that is, control (CN), MCI, and AD groups.

According to the findings of several studies, atrophy in the brain of AD patients is due to the accumulation of Aβ plaques (15). Besides the impact of amyloid plaques and neurofibrillary tangles in the brain, our investigation of the correlation between rCBF and structural changes of the brain might suggest a different pathological pathway, involved in the brain cortical and subcortical changes. Overall, further investigations can reveal the possible role of reduced rCBF in the structural changes of cortical and subcortical regions of the brain.

Materials And Methods

Data acquisition

The participants' information was collected from the Alzheimer's Disease Neuroimaging Initiative (ADNI) database (adni.loni.usc.edu). The ADNI, which was led by the principal investigator, Michael W. Weiner (MD), was launched in 2003 as a public-private partnership. The primary goal of ADNI was to determine whether serial MRI, positron emission tomography (PET), biological marker examinations, and clinical/neuropsychological assessments can be combined to measure the progression of MCI and early AD. A total of 149 subjects, including 28 patients with diagnosed AD, 82 MCI patients, and 39 healthy subjects from the ADNI, were recruited in this study. The diagnostic status, Mini-Mental State Examination (MMSE) score, and the result of apolipoprotein E gene (APOE) genotyping for each subject were available in the ADNI. All patients with available imaging results were enrolled in this study.

MRI processing

In this study, volumetric segmentation was carried out using FreeSurfer, which is available for download online (http://surfer.nmr.mgh.harvard.edu/). The processing consisted of motion correction of multiple T1-weighted images, removal of non-brain tissues, automated Talairach transformation, segmentation of subcortical white matter and gray matter structures, automated topology correction, and intensity normalization. The ADNIGO and ADNI2 were run in FreeSurfer version 5.1. In ADNIGO, an accelerated T1 image and a non-accelerated T1 image were acquired for each subject. Both images were pre-processed by Mayo Clinic. Processing consisted of three steps: Autorecon-1 command, which initiates multiple tasks, such as motion correction, non-uniform (NU) intensity normalization, Talairach transform computation, intensity normalization 1, and skull stripping; Autorecon-2 command, which creates white matter and pial surfaces and is involved in the segmentation of grey and white matter structures; and autorecon-3, which creates the cortical parcellation.

Arterial spin labeling (ASL)-MRI processing

In this study, ASL, as a completely non-invasive procedure, was used to measure the CBF by exploiting the endogenous spins of arterial water as a proxy for blood flow. Also, labeling magnetization of arterial spins was inverted selectively. The Center for Imaging of Neurodegenerative Diseases (CIND) prepared perfusion-weighted images (PWI), computed a map of CBF, and conducted a regional analysis. Overall, the ASL-MRI pre-processing consisted of three steps. The first step involved motion correction, where ASL images were converted from DICOM to NiFTI format. In the next step, PWI computations were done. The ASL images were separated into two groups of tagged and untagged, and the mean of each group was computed and saved. Next, to obtain the PWI, the difference in the mean of the two groups was determined. The first untagged image was used as the reference for water density and termed “M0”. M0 was used to calibrate the ASL signal for CBF computations and estimate the transformation from ASL-MRI and structural MRI as an intermediate frame. The third step was intensity scaling of PWI, as well as the M0 image. The detailed procedure is available online (adni.loni.usc.edu).

Statistical analysis

Before the statistical analysis, variables without a normal distribution were log-transformed to meet the normality assumption. Demographic variables were compared between the groups using the ANOVA test. Local associations between the rCBF and structural variables were investigated using correlation models. Partial correlation models were implemented for each association separately by adding rCBF and structural variables (i.e., subcortical and cortical volume, thickness, and surface area) for each region and entering age, sex, and APOE-ε4 genotyping status as controlled variables. The bootstrapping method was used for addressing type I errors due to multiple comparisons. The significance level was set at 0.05, and statistical analysis was performed in SPSS version 16.

Results

Participants’ characteristics

Table 1 shows the demographic data of the participants. There was no significant difference in terms of age, education, and sex between the groups. The AD group had significantly lower MMSE scores and more APOE-ε4 carriers as compared to the other groups.

Local correlation between rCBF and subcortical volume

After implementing controlled correlation models, we found a significant local correlation between the rCBF and subcortical volume in the groups. In the AD group, only a local correlation was found in the fourth ventricle, whereas in the MCI group, local correlations were observed in the third and fourth left and right lateral ventricles, as well as the right nucleus accumbens (Table 2). Also, significant correlations were observed in the right pallidum, right vessel, and white matter of the left hemisphere cerebellum in the CN group (Table 2).

Local correlation between rCBF and thickness

In all AD patients, negative correlations were only found in two regions, that is, the posterior segment of the left middle frontal gyrus and the caudal part of the right anterior cingulate cortex (Table 3, Figure 1). The results of Pearson's correlation test showed a correlation between the rCBF and thickness in many regions in the MCI group (Table 3, Figure 1). Significant correlations were also observed in the left entorhinal area, left and right lateral occipital cortices, left and right superior parietal lobules, right inferior parietal lobule, posterior part of the right middle frontal gyrus, right superior frontal gyrus, right inferior temporal gyrus, right pericalcarine, right postcentral gyrus, right precentral gyrus, and rostral part of the right anterior cingulate cortex (Table 3, Figure 1). Finally, in healthy subjects, a correlation was found in the left entorhinal area and the rostral part of the left anterior cingulate cortex (Table 3, Figure 1).

Local correlation between rCBF and cortical volume

The results demonstrated a significant correlation between the rCBF and cortical volume only in the MCI and CN groups (Table 4, Figure 1). In the MCI group, significant positive correlations were observed in the following regions: left and right postcentral gyrus, left and right precentral gyrus, left and right precuneus, right precuneus, left and right posterior cingulate cortex, caudal and rostral parts of the left anterior cingulate, right superior frontal gyrus, left and right superior parietal lobules, right inferior parietal lobule, left and right superior temporal gyri, right transverse temporal gyrus, left and right inferior temporal gyri, left middle temporal gyrus, left temporal gyrus, right lateral occipital gyrus, left and right supramarginal gyri, right insula, left entorhinal cortex, and right bankssts (Table 4, Figure 1). Significant correlations were fewer in the CN group, involving the left and right superior parietal gyri, right supramarginal gyrus, left entorhinal cortex, left fusiform gyrus, left medial orbital gyrus, anterior part of the left middle frontal gyrus, left temporal gyrus, right inferior temporal gyrus, and rostral part of the left anterior cingulate cortex (Table 4, Figure 1). However, there was no significant correlation in AD patients.

Local correlation between rCBF and surface area

Investigation of the local association between the rCBF and surface area in the groups revealed that in AD patients, this correlation was present in the left inferior temporal gyrus and isthmus of the left cingulate gyrus (Table 5, Figure 1). As shown in Table 5, significant correlations in the MCI group were more than other groups, similar to previous models (Table 5, Figure 1). The rCBF and surface area were correlated in the following regions in MCI patients: the left and right precuneus, right superior and inferior parietal lobules, right superior temporal gyrus, left and right transverse temporal gyri, left inferior and middle temporal gyri, left temporal pole, caudal and rostral parts of the left anterior cingulate gyrus, left posterior cingulate gyrus, left supramarginal gyrus, right middle orbital gyrus, right bankssts, and right fusiform gyrus (Table 5, Figure 1).

Moreover, in the CN group, significant correlations were observed in the following regions: the right precentral gyrus, left and right superior parietal lobules, left and right supramarginal gyri, left fusiform gyrus, left and right lateral occipital gyri, right inferior and middle temporal gyri, and the orbital part of the left inferior frontal gyrus (Table 5, Figure 1).

Discussion

Our findings revealed a significant correlation between the rCBF and structural changes, including cortical volume, subcortical volume, surface area, and thickness in all groups after adjusting for age, sex, and APOE genotyping status. To the best of our knowledge, this is the first study investigating the correlation between the rCBF and structural changes, including cortical volume, subcortical volume, and surface area in patients with cognitive impairments.

Recently, Kim et al. revealed no significant association between the rCBF and thickness in MCI patients and healthy people (16). Generally, the CBF decline is one of the earliest events in patients with AD (17). Evidence on CBF changes in patients with MCIs revealed that an increase or decrease in perfusion can be an early marker of neurodegeneration and may reflect metabolic demand changes in regions that are involved in cognitive function, including the temporal lobe, parietal lobe, frontal lobe, posterior cingulate gyrus, and precuneus (18, 19). Also, alterations in cortical and subcortical regions, especially in the medial temporal lobe, have been observed, which are thought to be an indirect marker of neuronal damage in the preclinical phase of AD and can be detected by MRI (20, 21). Moreover, cortical and subcortical volume, surface area, and thickness may help diagnose AD and accurately predict the cognitive decline as a result of neurodegeneration (22, 23).

Our findings revealed that changes in the rCBF can predict structural changes in various brain regions, including the cortical and subcortical areas, in AD, MCI, and healthy individuals. The correlations were mostly found in the medial temporal, temporal, parietal, occipital, and frontal regions, which are thought to be sensitive areas for the early pathology of AD (24). More involved regions were detected in our study, including the precentral gyrus, pericalcarine cortex, entorhinal cortex, supramarginal gyrus, fusiform, pallidum, and ventricles. Notably, we found a correlation between the rCBF and cortical volume and surface area in the posterior cingulate cortex and temporal pole of MCI patients, which are the main regions in the default mode network (DMN) (25). It should be mentioned that this association was mostly observed in the preclinical stage of AD, according to our results.

Generally, the decline in CBF leads to brain dysfunction, structural changes in the AD pathogenesis, and even death (26). According to our results, the rCBF may be responsible for further structural changes and atrophy in the pathogenic course of AD; however, the mechanism of hypoperfusion in the early stages of neurodegeneration is unclear. Evidence shows that the rCBF decline can lead to Aβ and hyperphosphorylated tau accumulation (26). On the other hand, some findings revealed that rCBF could be result of Aβ pathology (27).

Studies suggest that Aβ can impair the fundamental mechanisms of blood supply regulation (28, 29). However, several factors might account for this dysregulation in AD, such as impairment of endothelium-dependent responses, hypercontractile phenotype of cerebral smooth muscle cells, and vascular oxidative stress (30). In this regard, Michels et al. observed a significant relationship between the rCBF and APOE-ε4, independent of Aβ accumulation in MCI and normal elderly individuals (31). Moreover, other studies

found rCBF alterations in the right parahippocampal gyrus, bilateral cingulate gyri, and frontal regions in APOE-ε4 carriers (18, 32).

We found strong correlations between the rCBF and structural changes in the main brain regions involved in AD development, including the cingulate gyrus, temporal gyrus, and parietal lobule, which differ between healthy individuals and patients with AD and MCI, according to recent studies (33, 34). Although the role of tau pathology in neurodegeneration seems to be stronger than Aβ, both are associated with early pathological changes in AD (35). According to our hypothesis, CBF may independently predict structural changes due to AD progression. However, it is still debatable whether the altered CBF is the cause or consequence of atrophy and structural changes (16).

In contrast to our findings, Luckhaus et al. found no significant association between atrophy and CBF in the early pathogenesis of AD (36). Conversely, another study reported a significant correlation between CBF and cortical thickness in the predementia stages (37). Another study investigated the patterns of atrophy and hypoperfusion in MCI patients, compared to the controls, and found that both cerebral perfusion and gray matter structure reduced in the entorhinal cortex and the isthmus cingulate cortex. However, in several regions, the CBF decline and atrophy were observed independently in MCI patients (38).

Conclusion

According to the present results, CBF, as measured by ASL-MRI, might predict future structural changes and cause neurodegeneration associated with AD development, regardless of Aβ or tau accumulation. However, there are some unresolved issues regarding the role of Aβ and tau pathologies in blood flow dysregulations and structural changes underlying the pathology of CBF in the AD mechanisms; therefore, further research is needed in this area.

Declarations

Data used in this article's preparation were obtained from the Alzheimer's Disease Neuroimaging Initiative (ADNI) database (adni.loni.usc.edu). The ADNI investigators contributed to the design and implementation of ADNI and/or provided data but did not participate in the analysis or writing of this report. A complete listing of ADNI investigators can be found at: http://adni.loni.usc.edu/wp-content/uploads/how_to_apply/ADNI_Acknowledgement_List.pdf

Declaration of Interest: None.

Acknowledgments

Data collection and sharing for this project was funded by the Alzheimer's Disease Neuroimaging Initiative (ADNI) (National Institutes of Health Grant U01 AG024904) and DOD ADNI (Department of Defense award number W81XWH-12-2-0012). ADNI is funded by the National Institute on Aging, the

National Institute of Biomedical Imaging and Bioengineering, and through generous contributions from the following: AbbVie, Alzheimer’s Association; Alzheimer’s Drug Discovery Foundation; Araclon Biotech; BioClinica, Inc.; Biogen; Bristol-Myers Squibb Company; CereSpir, Inc.; Cogstate; Eisai Inc.; Elan Pharmaceuticals, Inc.; Eli Lilly and Company; EuroImmun; F. Hoffmann-La Roche Ltd and its affiliated company Genentech, Inc.; Fujirebio; GE Healthcare; IXICO Ltd.; Janssen Alzheimer Immunotherapy Research & Development, LLC.; Johnson & Johnson Pharmaceutical Research & Development LLC.; Lumosity; Lundbeck; Merck & Co., Inc.; Meso Scale Diagnostics, LLC.; NeuroRx Research; Neurotrack Technologies; Novartis Pharmaceuticals Corporation; Pfizer Inc.; Piramal Imaging; Servier; Takeda Pharmaceutical Company; and Transition Therapeutics. The Canadian Institutes of Health Research is providing funds to support ADNI clinical sites in Canada. Private sector contributions are facilitated by the Foundation for the National Institutes of Health (www.fnih.org). The grantee organization is the Northern California Institute for Research and Education, and the study is coordinated by the Alzheimer’s Therapeutic Research Institute at the University of Southern California. ADNI data are disseminated by the Laboratory for Neuro Imaging at the University of Southern California.

References

1. Burns A, Iliffe S. Alzheimer's disease. BMJ (Online). 2009;338(7692):467-71.
2. Johnson KA, Fox NC, Sperling RA, Klunk WE. Brain imaging in Alzheimer disease. Cold Spring Harbor perspectives in medicine. 2012;2(4):a006213-a.
3. Vemuri P, Whitwell JL, Kantarci K, Josephs KA, Parisi JE, Shiung MS, et al. Antemortem MRI based STructural Abnormality iNDex (STAND)-scores correlate with postmortem Braak neurofibrillary tangle stage. NeuroImage. 2008;42(2):559-67.
4. Pini L, Pievani M, Bocchetta M, Altomare D, Bosco P, Cavedo E, et al. Brain atrophy in Alzheimer's Disease and aging. Ageing Research Reviews. 2016;30:25-48.
5. Dubois B, Feldman HH, Jacova C, Cummings JL, Dekosky ST, Barberger-Gateau P, et al. Revising the definition of Alzheimer's disease: a new lexicon. 2010. p. 1118-27.
6. Whitwell JL. Progression of Atrophy in Alzheimer ’ s Disease and Related Disorders. 2010:339-46.
7. Berron D, van Westen D, Ossenkoppele R, Strandberg O, Hansson O. Medial temporal lobe connectivity and its associations with cognition in early Alzheimer's disease. Brain. 2020;143(3):1233-48.
8. Stranahan AM, Mattson MP. Selective vulnerability of neurons in layer II of the entorhinal cortex during aging and Alzheimer's disease. Neural Plasticity. 2010;2010.
9. Scheff SW, Price DA, Ansari MA, Roberts KN, Schmitt FA, Ikonomovic MD, et al. Synaptic change in the posterior cingulate gyrus in the progression of Alzheimer's disease. Journal of Alzheimer's Disease. 2015;43(3):1073-90.
10. Bejanin A, La Joie R, Landeau B, Belliard S, De La Sayette V, Eustache F, et al. Distinct Interplay between Atrophy and Hypometabolism in Alzheimer's Versus Semantic Dementia. Cerebral Cortex. 2019;29(5):1889-99.

11. Camarda C, Torelli P, Pipia C, Battaglini I, Azzarello D, Rosano R, et al. Association Between Atrophy of the Caudate Nuclei, Global Brain Atrophy, Cerebral Small Vessel Disease and Mild Parkinsonian Signs in Neurologically and Cognitively Healthy Subjects Aged 45-84 Years: A Crosssectional Study. Current Alzheimer research. 2018;15(11):1013-26.
12. Burton EJ, McKeith IG, Burn DJ, Williams ED, O'Brien JT. Cerebral atrophy in Parkinson's disease with and without dementia: a comparison with Alzheimer's disease, dementia with Lewy bodies and controls. Brain : a journal of neurology. 2004;127(Pt 4):791-800.
13. Weiler M, Agosta F, Canu E, Copetti M, Magnani G, Marcone A, et al. Following the spreading of brain structural changes in Alzheimer's disease: A longitudinal, multimodal MRI study. Journal of Alzheimer's Disease. 2015;47(4):995-1007.
14. Korte N, Nortley R, Attwell D. Cerebral blood flow decrease as an early pathological mechanism in Alzheimer's disease. Acta Neuropathologica. 2020;140(6):793-810.
15. Mattsson N, Tosun D, Insel PS, Simonson A, Jack CR, Beckett LA, et al. Association of brain amyloid-β with cerebral perfusion and structure in Alzheimer's disease and mild cognitive impairment. Brain. 2014;137(5):1550-61.
16. Kim CM, Alvarado RL, Stephens K, Wey HY, Wang DJJ, Leritz EC, et al. Associations between cerebral blood flow and structural and functional brain imaging measures in individuals with neuropsychologically defined mild cognitive impairment. Neurobiology of aging. 2020;86:64-74.
17. Shirayama Y, Takahashi M, Oda Y, Yoshino K, Sato K, Okubo T, et al. rCBF and cognitive impairment changes assessed by SPECT and ADAS-cog in late-onset Alzheimer's disease after 18 months of treatment with the cholinesterase inhibitors donepezil or galantamine. Brain imaging and behavior. 2019;13(1):75-86.
18. Wierenga CE, Dev SI, Shin DD, Clark LR, Bangen KJ, Jak AJ, et al. Effect of mild cognitive impairment and APOE genotype on resting cerebral blood flow and its association with cognition. Journal of cerebral blood flow and metabolism : official journal of the International Society of Cerebral Blood Flow and Metabolism. 2012;32(8):1589-99.
19. Wolk DA, Detre JA. Arterial spin labeling MRI: an emerging biomarker for Alzheimer's disease and other neurodegenerative conditions. Current opinion in neurology. 2012;25(4):421-8.
20. Pettigrew C, Soldan A, Zhu Y, Wang M-C, Moghekar A, Brown T, et al. Cortical thickness in relation to clinical symptom onset in preclinical AD. Neuroimage Clin. 2016;12:116-22.
21. Parker TD, Slattery CF, Zhang J, Nicholas JM, Paterson RW, Foulkes AJM, et al. Cortical microstructure in young onset Alzheimer's disease using neurite orientation dispersion and density imaging. Human brain mapping. 2018;39(7):3005-17.
22. Li C, Wang J, Gui L, Zheng J, Liu C, Du H. Alterations of whole-brain cortical area and thickness in mild cognitive impairment and Alzheimer's disease. Journal of Alzheimer's disease : JAD. 2011;27(2):281-90.
23. Lee YW, Lee H, Chung IS, Yi HA. Relationship between postural instability and subcortical volume loss in Alzheimer's disease. Medicine. 2017;96(25):e7286.

24. Leandrou S, Petroudi S, Kyriacou PA, Reyes-Aldasoro CC, Pattichis CS. Quantitative MRI Brain Studies in Mild Cognitive Impairment and Alzheimer's Disease: A Methodological Review. IEEE reviews in biomedical engineering. 2018;11:97-111.
25. Buckner RL, Andrews-Hanna JR, Schacter DL. The brain's default network: anatomy, function, and relevance to disease. Annals of the New York Academy of Sciences. 2008;1124:1-38.
26. Moskowitz MA, Lo EH, Iadecola C. The science of stroke: mechanisms in search of treatments. Neuron. 2010;67(2):181-98.
27. Park L, Anrather J, Zhou P, Frys K, Pitstick R, Younkin S, et al. NADPH-oxidase-derived reactive oxygen species mediate the cerebrovascular dysfunction induced by the amyloid beta peptide. J Neurosci. 2005;25(7):1769-77.
28. Niwa K, Younkin L, Ebeling C, Turner SK, Westaway D, Younkin S, et al. Abeta 1-40-related reduction in functional hyperemia in mouse neocortex during somatosensory activation. Proceedings of the National Academy of Sciences of the United States of America. 2000;97(17):9735-40.
29. Niwa K, Kazama K, Younkin L, Younkin SG, Carlson GA, Iadecola C. Cerebrovascular autoregulation is profoundly impaired in mice overexpressing amyloid precursor protein. American journal of physiology Heart and circulatory physiology. 2002;283(1):H315-23.
30. Chow N, Bell RD, Deane R, Streb JW, Chen J, Brooks A, et al. Serum response factor and myocardin mediate arterial hypercontractility and cerebral blood flow dysregulation in Alzheimer's phenotype. Proceedings of the National Academy of Sciences of the United States of America. 2007;104(3):823-8.
31. Michels L, Warnock G, Buck A, Macauda G, Leh SE, Kaelin AM, et al. Arterial spin labeling imaging reveals widespread and Aβ-independent reductions in cerebral blood flow in elderly apolipoprotein epsilon-4 carriers. Journal of cerebral blood flow and metabolism : official journal of the International Society of Cerebral Blood Flow and Metabolism. 2016;36(3):581-95.
32. Kim SM, Kim MJ, Rhee HY, Ryu CW, Kim EJ, Petersen ET, et al. Regional cerebral perfusion in patients with Alzheimer's disease and mild cognitive impairment: effect of APOE epsilon4 allele. Neuroradiology. 2013;55(1):25-34.
33. Cheng CP, Cheng ST, Tam CW, Chan WC, Chu WC, Lam LC. Relationship between Cortical Thickness and Neuropsychological Performance in Normal Older Adults and Those with Mild Cognitive Impairment. Aging and disease. 2018;9(6):1020-30.
34. Yi HA, Möller C, Dieleman N, Bouwman FH, Barkhof F, Scheltens P, et al. Relation between subcortical grey matter atrophy and conversion from mild cognitive impairment to Alzheimer's disease. Journal of neurology, neurosurgery, and psychiatry. 2016;87(4):425-32.
35. Montal V, Vilaplana E, Alcolea D, Pegueroles J, Pasternak O, González-Ortiz S, et al. Cortical microstructural changes along the Alzheimer's disease continuum. Alzheimer's & dementia : the journal of the Alzheimer's Association. 2018;14(3):340-51.
36. Luckhaus C, Cohnen M, Flüss MO, Jänner M, Grass-Kapanke B, Teipel SJ, et al. The relation of regional cerebral perfusion and atrophy in mild cognitive impairment (MCI) and early Alzheimer's

dementia. Psychiatry research. 2010;183(1):44-51.

37. Lacalle-Aurioles M, Mateos-Pérez JM, Guzmán-De-Villoria JA, Olazarán J, Cruz-Orduña I, Alemán-Gómez Y, et al. Cerebral blood flow is an earlier indicator of perfusion abnormalities than cerebral blood volume in Alzheimer's disease. Journal of cerebral blood flow and metabolism : official journal of the International Society of Cerebral Blood Flow and Metabolism. 2014;34(4):654-9.
38. Wirth M, Pichet Binette A, Brunecker P, Köbe T, Witte AV, Flöel A. Divergent regional patterns of cerebral hypoperfusion and gray matter atrophy in mild cognitive impairment patients. Journal of cerebral blood flow and metabolism : official journal of the International Society of Cerebral Blood Flow and Metabolism. 2017;37(3):814-24.

Tables

TABLE1. Participants characteristic

Demographic and health characteristic	CN(39)	MCI(82)	AD(28)	P value
Age, years	71.8(±6.8)	70.4(±7.4)	73.1 (±6.5)	0.186
Sex(M/F)	15/24	41/41	14/14	0.469
Education, years	16.2(±2.5)	16.5(2.7)	16.5(±2.2)	0.829
MMSE	28.9(±1.4)	28.3(±1.6)	23.9(±1.9)	0.000
APOE genotype				0.000
With out ε4	26	53	8	
One ε4	11	22	12	
Two ε4	1	7	8	

Values are showed as mean(±SD), Mini Mental State Examination(MMSE), results of One way ANOVA analysis between groups noted as p value

TABLE2. Significant Results of partial Correlation Analyses of CBF and subcortical volume within groups

Regions	Correlation coefficient	P value
AD		
4^{th} Ventricle	-0.529	0.007
MCI		
4^{th} Ventricle	-0.249	0.029
Left lateral ventricle	-0.346	0.002
Right lateral ventricle	-0.231	0.043
Right nucleus accumbens	0.244	0.030
3^{th} Ventricle	-0.263	0.021
CN		
White matter of left hemisphere cerebellum	0.596	0.000
Right pallidum	0.512	0.002
Right vessel	0.431	0.010

Cerebral blood flow (CBF), Alzheimer's disease (AD), mild cognitive impairment (MCI), control normal (CN)

TABLE3. Significant Results of partial Correlation Analyses of CBF and Thickness within groups

Regions	Correlation coefficient	P value
AD		
Posterior part of left middle frontal	-0.457	0.033
Caudal part of right anterior cingulate	-0.544	0.005
MCI		
Left entorhinal area	0.237	0.035
Left lateral occipital	0.259	0.022
Right lateral occipital	0.284	0.012
Left superior parietal lobule	0.250	0.026
Right superior parietal	0.357	0.001
Posterior part of right middle frontal	0.288	0.010
Right inferior parietal lobule	0.316	0.005
Right inferior temporal	0.299	0.011
Right pericalcarine	0.234	0.039
Right postcentral	0.231	0.040
Right precentral	0.307	0.006
Rostral part of right anterior cingulate	-0.243	0.031
Right superior frontal	0.303	0.007
CN		
Left entorhinal area	0.400	0.017
Rostral part of left anterior cingulate	0. 523	0.001

Cerebral blood flow (CBF), Alzheimer’s disease (AD), mild cognitive impairment (MCI), control normal (CN)

TABLE4. Significant Results of partial Correlation Analyses of CBF and Cortical volume within groups

Regions	Correlation coefficient	P value
MCI		
Right postcentral	0.284	0.011
Right posterior cingulate	0.234	0.038
Right precentral	0.286	0.011
Right precuneus	0.387	0.000
Right superior frontal	0.248	0.027
Right superior parietal	0.372	0.001
Right superior temporal	0.257	0.029
Right supramarginal	0.266	0.018
Right transverse temporal	0.244	0.030
Right insula	0.255	0.023
Caudal part of left anterior cingulate	0.272	0.015
Left entorhinal	0.301	0.007
Left inferior temporal	0.244	0.039
left middle temporal	0.302	0.010
Left paracentral	0.264	0.019
Left postcentral	0.268	0.017
Left posterior cingulate	0.256	0.023
Left precentral	0.288	0.010
Left precuneus	0.360	0.001
Rostral part of left anterior cingulate	0.372	0.001
Left superior parietal	0.297	0.008
Left superior temporal	0.268	0.023
Left supramarginal	0.320	0.004
Left temporal	0.296	0.012
right bankssts	0.258	0.022
Right inferior parietal	0.460	0.000
Right inferior temporal	0.351	0.003
Right lateral occipital	0.274	0.015
CN		
Right superior parietal	0.348	0.041

Right supramarginal	0.346	0.042
Left entorhinal	0.383	0.023
Left fusiform	0.401	0.021
Left medial orbital	0.385	0.022
Anterior part of left middle frontal	0.374	0.027
Left superior parietal	0.412	0.014
Left temporal	0.368	0.035
Right inferior temporal	0.406	0.019
Rostral part of left anterior cingulate	0. 523	0.001

Cerebral blood flow (CBF), Alzheimer’s disease (AD), mild cognitive impairment (MCI), control normal (CN)

TABLE5. Significant Results of partial Correlation Analyses of CBF and Surface area within groups

Regions	Correlation coefficient	P value
AD		
Left inferior temporal	0.441	0.031
Isthmus of left cingulate	0.458	0.021
MCI		
Right precuneus	0.315	0.005
Right superior parietal	0.254	0.024
Right superior temporal	0.279	0.018
Right transverse temporal	0.243	0.031
Caudal part of left anterior cingulate	0.367	0.001
Left inferior temporal	0.238	0.044
left middle temporal	0.283	0.016
Left posterior cingulate	0.249	0.027
Left precuneus	0.312	0.005
Rostral part of left anterior cingulate	0.387	0.000
Left supramarginal	0.297	0.008
Left temporal pole	0.259	0.028
Left transverse temporal	0.252	0.025
Right bankssts	0.282	0.012
Right fusiform	0.274	0.020
Right inferior parietal	0.338	0.002
Right middle orbital	0.269	0.017
CN		
Right precentral	0.379	0.025
Right superior parietal	0.411	0.014
Right supramarginal	0.383	0.023
Left fusiform	0.458	0.007
Left lateral occipital	0.388	0.021
Orbital part of left inferior frontal	0.385	0.022
Left superior parietal	0.441	0.008
Left supramarginal	0.388	0.021
Right inferior temporal	0.415	0.016

Right lateral occipital	0.498	0.002
Right middle temporal	0. 456	0.008

Cerebral blood flow (CBF), Alzheimer’s disease (AD), mild cognitive impairment (MCI), control normal (CN)

Figures

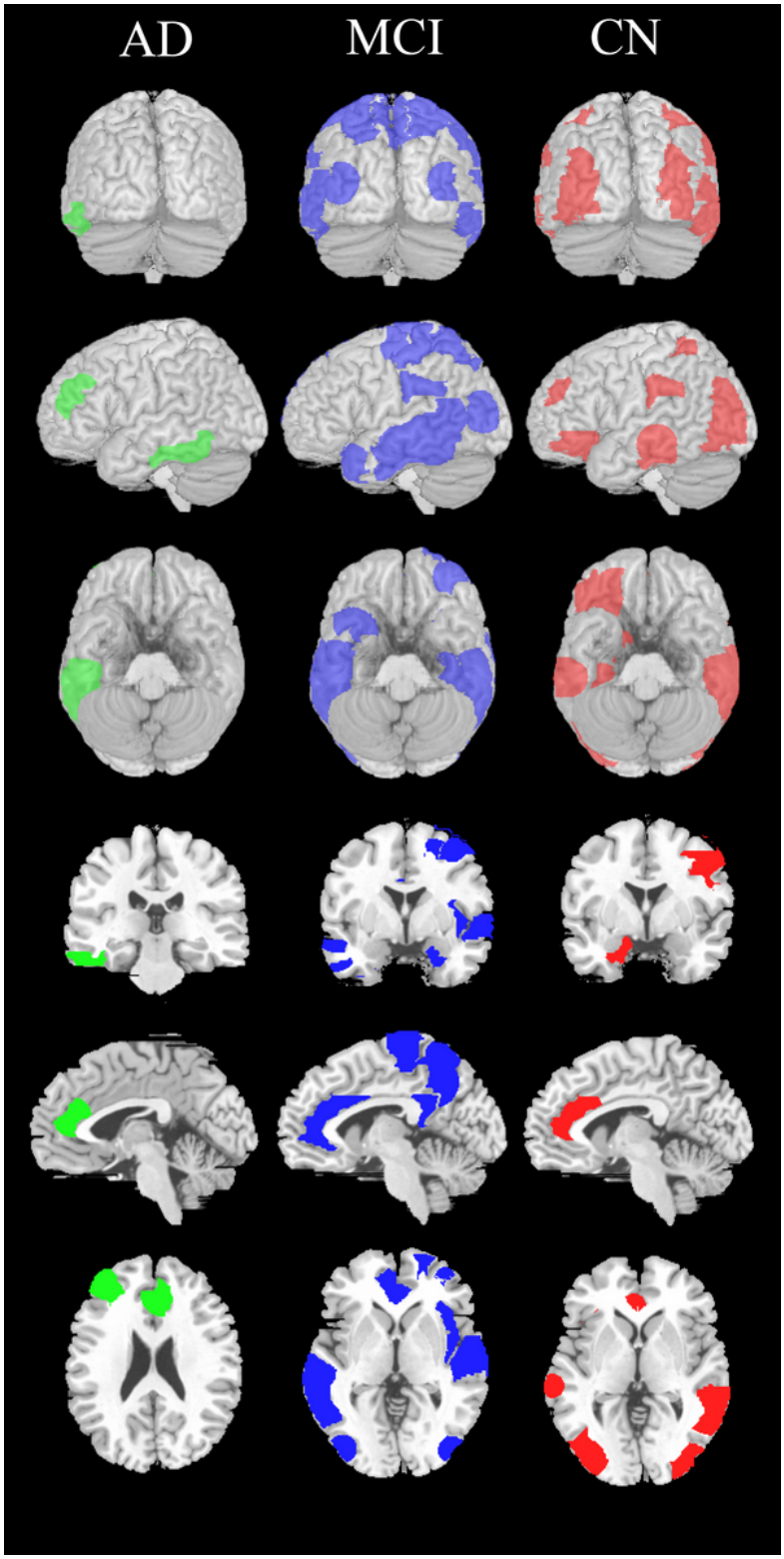

Figure 1

Regions of interest are shown for significant correlation between structural values and regional cerebral blood flow. AD (green), MCI (blue), CN (red). Alzheimer's Disease (AD), mild cognitive impairment (MCI), control (CN)